

# The background oriented schlieren technique: sensitivity, accuracy, resolution and application to a three-dimensional density field

Erik Goldhahn · Jörg Seume

Received: 29 September 2006 / Revised: 11 May 2007 / Accepted: 17 May 2007 / Published online: 10 July 2007  
© Springer-Verlag 2007

**Abstract** Three-dimensional density information of a double free air jet was acquired using optical tomography. The projections of the density field were measured using the background oriented schlieren method (BOS). Preceding the free jet measurements, the sensitivity, accuracy and resolution of the BOS method were investigated. The sensitivity depends mostly on the focal length of the lens used, the relative position of the object between camera and background and the smallest detectable shift in the image plane. The accuracy was found to be sufficiently high to apply a tomographic reconstruction process. The resolution is determined by the transfer function of the BOS-method. It is not constant and depends on the size of the interrogation windows used for the cross-correlation-algorithm. The reconstruction of the free jet was computed, using filtered back projection. The reconstructed 3D density field shows with good resolution the typical diamond structure of the density distribution in under-expanded free jets.

## List of symbols

$f$	focal length (m)
$g$	overall length of a BOS-set-up (m)
$h$	size of an interrogation window
$K$	Gladstone–Dale-constant
$k$	polar coordinate in the Fourier plane

$l$	distance between background and phase object (m)
$M$	magnification
$m$	distance between camera lens and phase object (m)
$n$	index of refraction
$p$	pressure (Pa)
$R$	gas constant [J/(kg K)]
$s$	coordinate in the polar coordinate system (m)
$T$	temperature (K)
$v_{px}$	shift in the sensor plane (m)
$v_H$	shift in the background (m)
$x, y, z$	Cartesian coordinates (m)
$x', y'$	auxiliary variable (m)

## Greek symbols

$\alpha$	Angle between reference light ray and measurement light ray
$\varepsilon$	Deflection angle of a light ray
$\theta$	Coordinate in the polar coordinate system
$\lambda$	spatial wavelength (m)
$\Pi$	Window function
$\rho$	Density (kg/m <sup>3</sup> )
$\varphi_{\text{tn}}$	Angle between light ray and line of sight

E. Goldhahn (✉) · J. Seume  
Institute of Turbomachinery and Fluid Dynamics,  
Leibniz University Hannover, Hannover, Germany  
e-mail: goldhahn@tfd.uni-hannover.de

J. Seume  
e-mail: seume@tfd.uni-hannover.de

## 1 Introduction

For the complete characterization of isothermal (e.g. cold free jets) or isobaric (e.g. flow in combustion chambers of gas turbines) flows, one thermodynamic state variable is needed in addition to the velocity field. In principle, this

information can be obtained by measuring the density or pressure distribution for isothermal flows or by measuring the density or temperature distribution for isobaric flows. The method presented here provides a means of measuring density fields.

In contrast to point measurements, optical field measurement methods have the advantage of capturing the complete flow field without disturbances due to probes inserted into the flow. For density measurements, methods belonging to the groups of shadowgraphy, schlieren techniques, and interferometry can be used. All of these methods are line of sight integrating techniques and are sensitive to changes of the refractive index of the investigated fluid. The paper of Dalziel et al. (2000) outlines some novel techniques for qualitative visualizations of density distributions. The BOS method used here belongs to the group of schlieren techniques and captures projections of the index of refraction gradient. It was proposed by Meier (1999). A comparison of this method to the calibrated color schlieren method can be found in the paper of Elsinga et al. (2004). Its applicability to different flow problems and even to full scale testing was demonstrated by Richard et al. (2000). Augenstein et al. (2001) used this technique for the visualization of the high speed flow around a canard wing configuration.

Due to the integrating character of the above mentioned measurement methods, local values of density cannot be determined directly. For phase objects with axial symmetry quantitative results can be derived from one projection using the Abel inversion technique. Klinge et al. (2003) used a single projection recorded with the BOS method and a simple recursion formula to determine the density field of a wing tip vortex. For objects with higher complexity more advanced tomographic reconstruction algorithms have to be employed. To collect the input data a number of projections of the measurement value must be recorded. The number of required projections depends on the complexity of the object. There are several studies regarding optical tomography in combination with classical density measurement methods (especially schlieren techniques and interferometry). Rottevel (1992) applied an interferometric method to the flow inside a combustion engine model, Blinkov et al. (1989) used multi-directional speckle photography to obtain the temperature distribution inside a candle flame and Faris et al. (1988) used beam-deflection optical tomography on a supersonic jet. The experimental complexity as well as the effort required to evaluate the measurements is very high for these methods. In contrast, the BOS method offers the possibility to record and evaluate projections from different viewing directions easily. It is also possible to capture different projection directions simultaneously using one camera for each direction. So far BOS was mostly used as a simple means for flow visualization. Some quantitative

investigations of 2D flows and flows with rotational symmetry have been carried out by Venkatakrisnan (2004) and Venkatakrisnan and Meier (2004). In both cases the authors used a Poisson equation to determine the projected (line-of-sight integrated) density field. This field was then used as the input data for a tomographic reconstruction algorithm (filtered back projection). This procedure is unnecessarily complex, since the projections taken with the BOS-Method are gradient information that can directly be fed into the filtered back projection algorithm, eliminating the need to integrate the line of sight projected density field. In this work the gradient information is used directly to reconstruct the density fields.

## 2 The BOS method

### 2.1 Measurement principle

A BOS set-up mainly consists of a camera, a computer to record and evaluate the images, and a background with a random dot pattern. The background is generated by an iterative procedure. In the first step, the dots are placed randomly on the background. In the second step each dot is checked for overlapping with neighboring dots. This procedure is repeated until the desired density of dots is reached. It allows generating round dots of defined size and density, which are all separated. That way the generated backgrounds can be optimally matched to the requirements of the subsequent correlation algorithms. In the present study, the density of the dots was chosen as high as possible using dots that give a dot image size of approximately 2.5 Pixel. By doing so, it is possible to have a large signal to noise ratio and a sub pixel accuracy of the shift data better than 0.1 Pixel. The influence of the dot size on the correlation result has been addressed by a number of authors, mainly concerned with PIV cross correlation algorithms. Since with BOS the same algorithms are used for the determination of the apparent shift, the results also apply to the present study. For more information about the influence of the dot size one may refer to M. Raffel et al. (1998).

The BOS method is, as all methods in the group of schlieren techniques sensitive to those components of the first spatial derivative of the index of refraction, which are perpendicular to the line of sight. The integral of these components along the line of sight can be determined with the BOS method using Eq. 1. For gases with  $n \approx 1$ , this equation can be used in a simplified version (Eq. 2).

$$\varepsilon \approx \tan(\varepsilon) = \sin(\varphi_m) \cdot \int_1 \frac{1}{n(x,y,z)} \text{grad}\{n(x,y,z)\} dt \quad (1)$$

$$\varepsilon \approx \tan(\varepsilon) = \sin(\varphi_m) \cdot \int_1 \text{grad}\{n(x,y,z)\} dt \tag{2}$$

$$n - 1 = K \cdot \rho. \tag{3}$$

Here  $t$  is the coordinate along the line of sight,  $\varepsilon$  is the deflection angle,  $\varphi_m$  is the angle between the line of sight and the direction of the gradient vector of the index of refraction, and  $n$  is the spatial distribution of the index of refraction. Variations of the index of refraction which are connected to the fluid density by the Gladstone–Dale relation (Eq. 3) cause an apparent shift ( $\Delta y$ ) of the background dot pattern as shown in Fig. 1.

Using cross-correlation algorithms these shifts can be evaluated through the comparison of a reference image (without flow) with a measurement image (with flow). From these shifts the deflection angles ( $\varepsilon$  in Eq. 2) of the light rays through the flow can be calculated using the geometric proportions of the set-up. In contrast to classical optical density measurement methods, BOS features a simple set-up, robustness, and independence from accurate intensity measurements. Therefore, it is especially suited for quantitative investigations. It can be used for the investigation of density fields, but also temperature, pressure, and concentration fields can be determined if in the first case the pressure, in the second case the temperature, and in the third case pressure and temperature are known a priori inside the field.

### 2.2 Sensitivity

Measurements using the BOS method are integral measurements. With BOS, the apparent shift of a background pattern is determined due to the refraction of light by a density gradient field. Using the geometric dimensions of the set-up and assuming the Angle  $\alpha$  to be small, the deflection angle  $\varepsilon$  in Eq. 2 can be calculated from that shift. It is related to the line of sight integral over the index of refraction gradients. Therefore the sensitivity question is

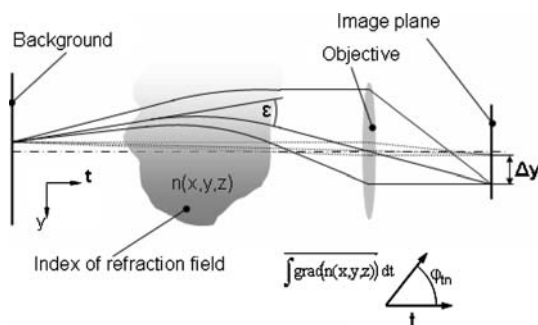


Fig. 1 BOS set-up (schematic)

linked to the question of the smallest detectable integral in Eq. 2.

Since the exact light path is dependent on the object under investigation and usually unknown, simplifications must be made in order to derive information about the sensitivity of a certain set-up. By concentrating the deflection of the light onto one plane in space, one obtains the geometric relations as in Fig. 2 (shown for one component of the index of refraction gradient).

From that Eq. 4 for the tangent of the deflection angle can be derived. By using Eq. 4 together with Eq. 5, the apparent background shift (Eq. 6) and the magnification (Eq. 7) one arrives at the relation in Eq. 8. Here  $f$  is the focal length of the lens,  $M$  the magnification factor,  $v_H$  the shift of the dots on the background, and  $v_{px}$  is the corresponding pixel shift on the sensor chip of the camera.

$$\tan(\varepsilon) = \frac{(1 + 1/m) \cdot \tan(\alpha)}{1/m - \tan^2(\alpha)} \tag{4}$$

$$\tan(\alpha) = \frac{v_H}{g} \cdot \cos^2(\beta) \tag{5}$$

$$v_H = \frac{v_{px}}{M} \tag{6}$$

$$M = \left(\frac{g}{f} - 1\right)^{-1} \tag{7}$$

$$\varepsilon \approx \tan(\varepsilon) = \sin(\varphi_m) \cdot \int_z \text{grad}(n(x,y,z))$$

$$dl = \frac{(1 + 1/m) \cdot v_{px} \left(\frac{g-f}{g \times f}\right) \cdot \cos^2(\beta)}{1/m - \left(v_{px} \left(\frac{g-f}{g \times f}\right) \cdot \cos^2(\beta)\right)^2} \tag{8}$$

With the assumption of Eq. 9, the result can be simplified further (Eq. 10).

$$\left(v_{px} \left(\frac{g-f}{g \times f}\right) \cdot \cos^2(\beta)\right)^2 \ll 1 \tag{9}$$

$$\varepsilon \approx (1 + m/l) \cdot v_{px} \left(\frac{g-f}{g \times f}\right) \cdot \cos^2(\beta). \tag{10}$$

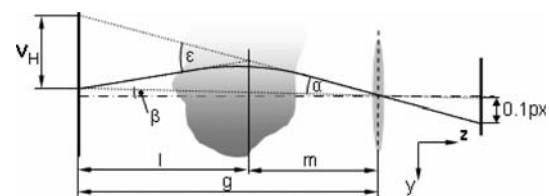


Fig. 2 Geometry for the sensitivity estimation

The deviation angle  $\beta$  is typically small so that the terms in italics in Eqs. 5–10 tend to 1 and therefore may be omitted in most cases.

Thus it is possible to estimate the sensitivity dependent on the parameters focal length of the lens, position of the object in the set-up, overall size of the set-up, and smallest detectable pixel shift. While the geometric properties are defined by the set-up, the smallest detectable pixel shift is dependent on the quality of the background as well as on the evaluation algorithms. Since the background dot pattern can be matched in pixel size and density to a certain set-up, it is possible to detect pixel shifts as small as 0.1 pixels with available cross-correlation algorithms. The pixel shift is linked to a certain physical shift through the resolution of the imaging sensor used.

Figure 3 shows the smallest detectable line of sight integral value (from Eq. 2) for three positions of the density object between camera and background. The smallest detectable pixel shift was set to 0.1 pixel for the camera used in the experiment (PCO Sensicam). The pixel size of that camera is  $6.7 \times 6.7 \mu\text{m}$ , giving a minimum detectable physical shift of 670 nm in the image plane. As can be seen in Fig. 3 the sensitivity increases with larger focal length as well as with a position of the object closer to the camera. In addition, higher resolution cameras will give a higher sensitivity, since the detectable physical shift on the sensor plane depends on the pixel size and the number of pixels on the sensor (if a constant field of view is assumed). In contrast, the overall length of the set-up plays a minor role and its influence comes only from the lens equation and the fact that the distances are referenced to the principal points of the lens. This can also be seen from Eq. 10 for the limiting case  $g \gg f$  and  $\beta = 0$  (Eq. 11).

$$\varepsilon \rightarrow (1 + m/l) \cdot \frac{v_{px}}{f}, \quad \text{for } g \gg f \tag{11}$$

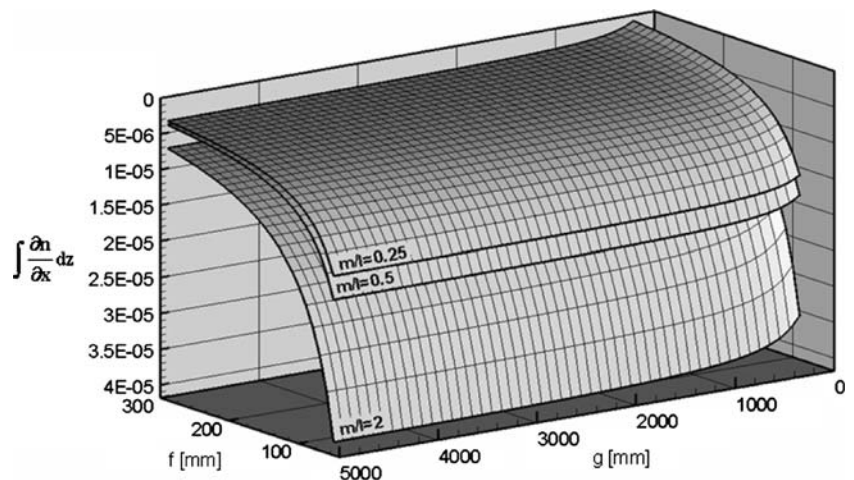
### 2.3 Accuracy

For the assessment of the accuracy of the BOS method, the density field of thermally stable stratified air has been investigated. The set-up is shown schematically in Fig. 4. It consists of a glass box of size of  $400 \text{ mm} \times 400 \text{ mm} \times 400 \text{ mm}$ . It is insulated at four sides and allows optical access through the two remaining, uninsulated faces. The glass box is electrically heated from the top in order to establish stable temperature stratification. The maximum heating power is 70 W. The maximum temperature gradient achievable with the set-up is 0.1 K/mm. The temperature level directly adjacent to the uninsulated glass faces is lower than in the rest of the box. Therefore the temperature gradients in  $x$ -direction are lower than in the rest of the box. But due to the good insulation characteristics of glass and air, this layer is thin compared to the overall length of the glass box. Its influence was estimated and turned out to be negligible. The temperature gradient in  $z$ -direction has no influence on the result, since the BOS-method is sensitive only to gradients perpendicular to the line of sight.

With that one obtains a density gradient field which is static and depends only on the distance to the heated top cover of the box. It can be measured by means of temperature sensors. Therefore, the glass box was equipped with six temperature sensors to determine the temperature profile simultaneously with the BOS measurements. The temperature readings of the temperature sensors were fitted by a spline function. From that function, the density gradients were calculated using Eq. 12, where  $R$  is the gas constant,  $p$  is the pressure, and  $x$  is the coordinate perpendicular to the heated cover plate.

$$\frac{\Delta\rho(x)}{\Delta x} = -\frac{p}{RT^2} \frac{\Delta T(x)}{\Delta x}. \tag{12}$$

**Fig. 3** Sensitivity for three different positions of the density object between camera and background (diagram drawn for a smallest detectable pixel shift of 0.1 px)



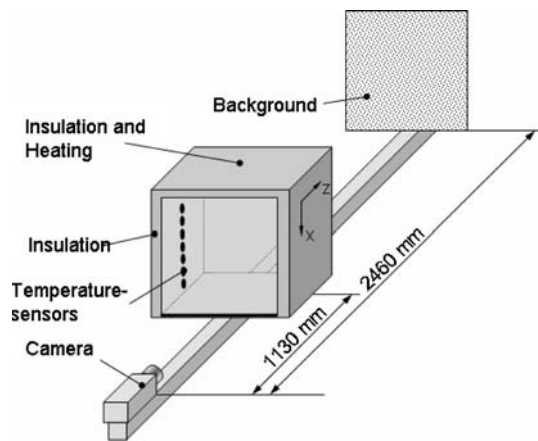


Fig. 4 Experimental set-up for the assessment of the accuracy

The accuracy of the temperature sensors for relative temperature measurements was  $\pm 0.1$  K. With that accuracy, the maximum error for the calculation of the density gradient amounts to  $\pm 1 \times 10^{-4}$  kg/m<sup>3</sup> mm.

To determine the deviation of the light rays from the apparent pixel shift, the optical set-up must be calibrated. Therefore a calibration grid was placed at the position of the background pattern. The calibration was done with the glass box in position. In that way, distortions from the lens and windows are accounted for in the calibration process. Assuming a 1D density distribution  $\rho(x)$ , the density gradients were calculated from the BOS data and compared to the gradients calculated from the temperature readings. The comparison shows good agreement (Fig. 5). It also shows that the accuracy of the BOS measurement is within the error margin of the temperature sensors, even for very low values of the density gradient.

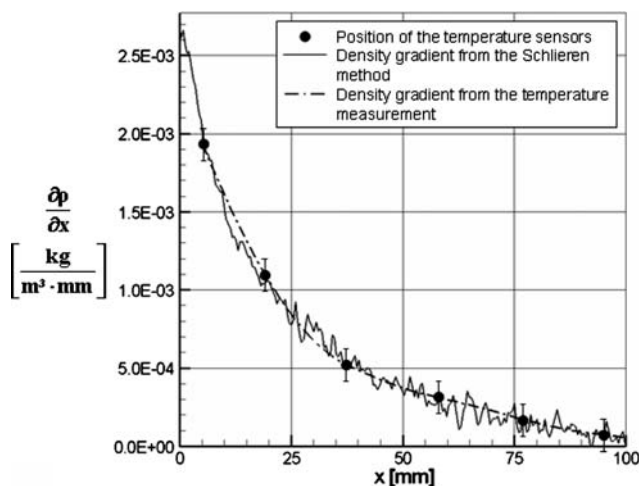


Fig. 5 Density gradient distribution from instantaneous BOS- and temperature measurements

### 2.4 Resolution

With BOS measurements, one obtains 2D projections of the 3D field of the index of refraction gradient. The information is contained in the apparent shift of the background pattern of the measurement image compared to the reference image. These projections are a continuous function of the projection coordinates. Therefore, it is not possible to distinguish between single objects as it is common in optics. But a definition of resolution can be found if one decomposes a projection into its harmonic components. Following this approach the resolution of a BOS set-up is the highest spatial frequency which can still be observed with the BOS system. It is therefore necessary to know the transfer function of the system. As described above, the information about the line of sight integral over the index of refraction gradients is contained in the apparent shift of the background pattern. This shift is calculated using cross-correlation algorithms. These algorithms are based on the recognition of the background intensity distribution in small areas (interrogation windows) in the reference and measurement images. The interrogation windows contain a limited number of randomly distributed dots. Therefore, strictly speaking, the shift calculated by cross correlation algorithms is an intensity-weighted mean shift per interrogation area. Considering the random overall distribution of the dots in the images, one can assume that the shift is averaged over the interrogation window size and overlaid with a certain amount of noise due to the distribution of the dots inside each interrogation window. With this assumption, it is possible to find a description for the transfer function of a BOS measurement.

Equation 13 describes the evaluation process for the apparent background shift as a moving average for rectangular interrogation windows. It is the 2D convolution of a window function with the projections of the index of refraction gradients divided by the window area. Equation 14 details the window function. In the Fourier space, this convolution equals the multiplication of the Fourier transform of the projections with the Fourier transform of the window function.

$$\begin{aligned} \left(\frac{\partial n}{\partial x}(x,y)\right)_{\text{mean}} &= \frac{1}{h^2} \int_{-\infty}^{\infty} \int_{-\infty}^{\infty} \frac{\partial n}{\partial x}(x',y') \cdot \\ &\prod(x-x',y-y')dx'dy' \\ \left(\frac{\partial n}{\partial y}(x,y)\right)_{\text{mean}} &= \frac{1}{h^2} \int_{-\infty}^{\infty} \int_{-\infty}^{\infty} \frac{\partial n}{\partial y}(x',y') \cdot \\ &\prod(x-x',y-y')dx'dy' \end{aligned} \tag{13}$$

$$\Pi(x,y) = \begin{cases} 1 & \text{für } |x| \leq \frac{h}{2} \wedge |y| \leq \frac{h}{2} \\ 0 & \text{für } |x| > \frac{h}{2} \vee |y| > \frac{h}{2} \end{cases} \quad (14)$$

Therefore the transfer function of the BOS evaluation is described by the amplitude spectrum of the window function. Figure 6 shows the transfer function for one frequency component. It influences the amplitude as well as the phase angle of the spatial frequencies of the decomposed shift distribution. Only the mean value of the shift in a projection is measured correctly. With integer multiples of the spatial wavelengths of the density gradients being equal to the interrogation window size, the values of the transfer function become zero. In between, the amplitudes corresponding to certain wavelengths of the decomposed projection are measured smaller than the real values.

This seems to be a major drawback of the method. But it is possible to reconstruct the true values of the projection data since the transfer function is known. The only exceptions are the values where the transfer function is zero. It is also possible to use iterative cross correlation algorithms as described for PIV-processing by Nogueira et al. (2005).

For the measurements in the free jet, which are described later, the effect of filtering by evaluating the projections with a cross correlation algorithm was not strong enough to influence the results significantly, because the interrogation windows were small compared to the smallest spatial wavelengths of significance in the region of interest.

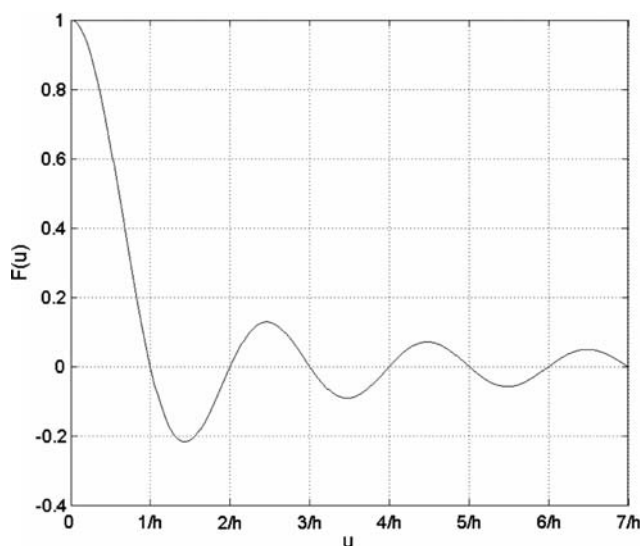


Fig. 6 Transfer function for one frequency component

### 3 Density measurement at a double free jet of air

#### 3.1 Experimental set-up

An under-expanded free jet of air is investigated. To create the jet, a simple double-hole orifice is used as shown in Fig. 7a. The orifice is mounted on a settling chamber equipped with rectifier screens for flow quality enhancement. The orifice can be turned after loosening four screws. It is equipped with an angular scale which allowed exact adjustment of the rotation angle in five steps. The holes have diameters of 5 and 15 mm, respectively. The center distance of the holes is 13 mm. The settling chamber is equipped with a port for total pressure readings and a sensor for total temperature. Both values are recorded together with the BOS measurements. Both, the camera and the background are supported by a stiff aluminum structure (Fig. 7b). The background is illuminated by a flash lamp, which is triggered together with the camera.

The shutter time of the camera is set to 5  $\mu$ s. The total pressure in the pre-chamber is held constant at 1.5 bar ( $\pm 0.02$  bar) above ambient pressure. With that set-up, 36 measurement directions are captured in succession with one camera. In each direction, 60 measurement images are taken. The images were evaluated using interrogation windows of the size 8 px by 8 px with 50% overlap. The Magnification factor was 5.03 px/mm. In every viewing direction the mean values of the shift data were calculated by averaging the correlation maps for each image as it is done in PIV-processing (Meinhart et al. (2000)). The 3D density field is determined using tomographic reconstruction with the averaged shift values.

#### 3.2 Tomographic reconstruction

The filtered back-projection algorithm was used for the reconstructions (see e.g. Formin 1997; Kak and Slaney 1988; Natterer 1986). The 3D density field was reconstructed in planes perpendicular to the jet axis. Parallel projection was assumed since the maximum opening angle of the used camera-lens combination was  $\pm 4^\circ$  and the free jet extended only over approximately  $\pm 2^\circ$ . The principle of the reconstruction process is shown in Fig. 8. From the apparent shift on the background the deflection angles are calculated. They correspond to the integral over the index of refraction gradients in Eq. 2. Taking that integral along a direction through the object to reconstruct gives a projection of the index of refraction gradients. From the center slice theorem and the derivative theorem it is known that the Fourier transform of the derivative of the projected values of a physical parameter (here the index of refraction  $n$ ) corresponds to the Fourier transform of the object itself in a slice through the Fourier plane. By taking enough

**Fig. 7** **a** Sketch of the double hole orifice **b** Experimental set up

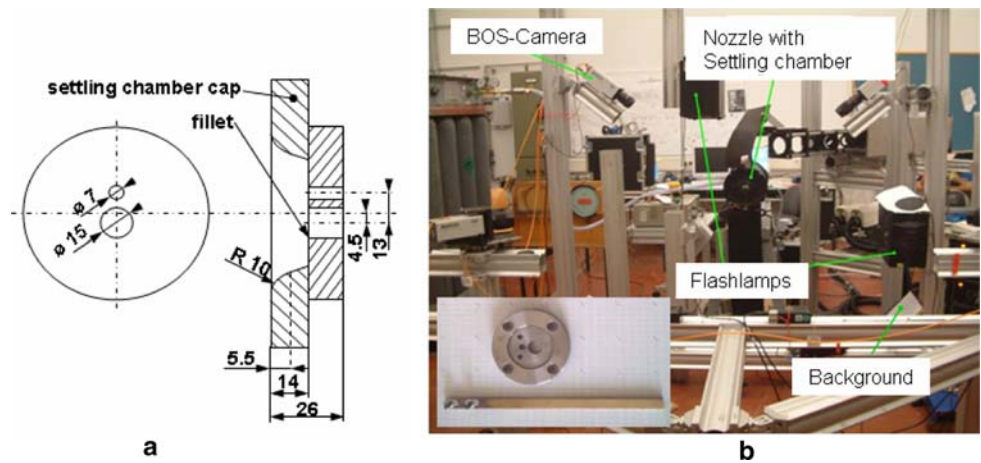
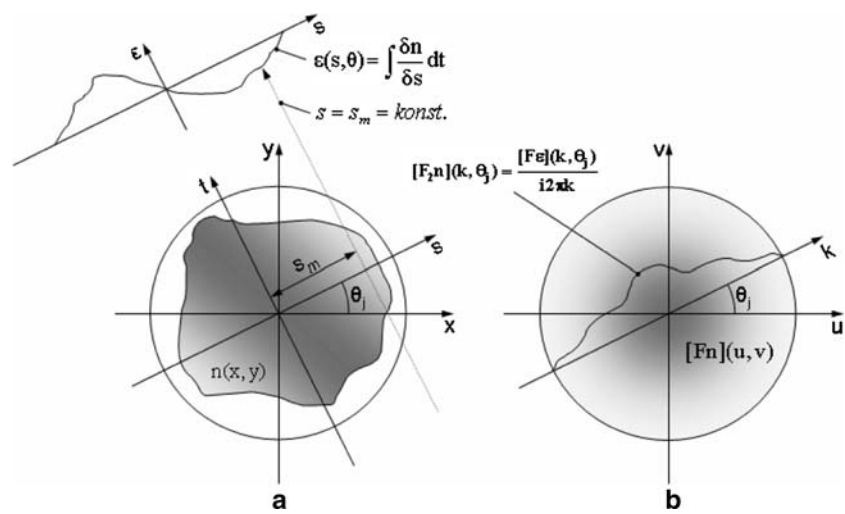


**Fig. 8** Principle of filtered back projection



projections through the object, the Fourier plane is successively filled with values which describe the object. Using the convolution theorem it is furthermore possible to compute the reconstruction entirely in the spatial domain. In this case the reconstruction is done by convolving the projections with an abs-filter (Eqs. 16, 17) and back projecting the result into the reconstruction area (Eq. 15).

$$n(x,y) = \int_0^\pi q(s) * \varepsilon_s(s, \theta) d\theta \tag{15}$$

$$\text{where } q(s) = \int_{-\infty}^\infty Q(k) e^{i2\pi ks} dk \tag{16}$$

$$\text{with } Q(k) = \frac{|k|}{i2\pi k} \tag{17}$$

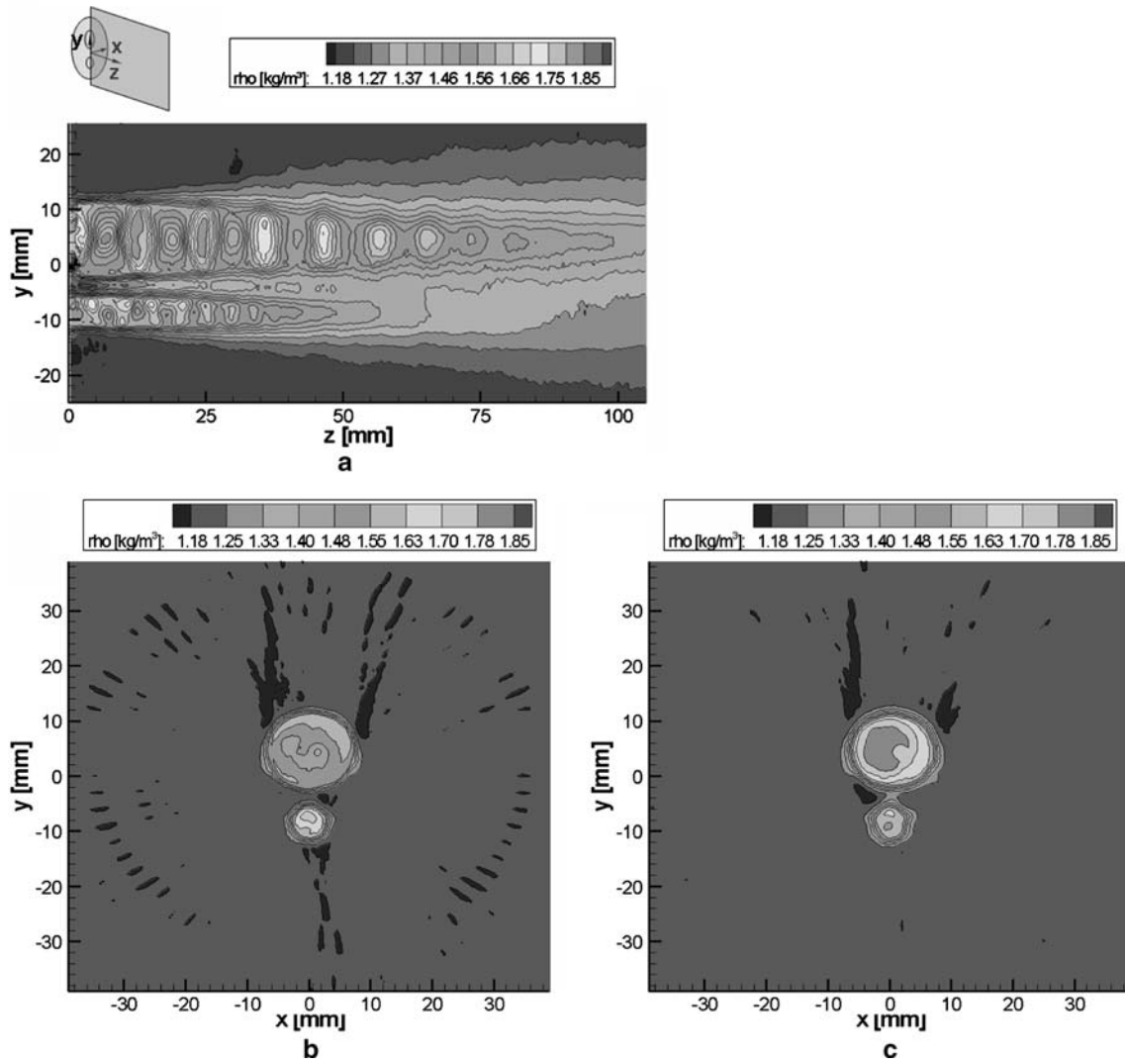
Doing so, one gets the index of refraction distribution in the first place. From the Gladstone–Dale relation, and the

ambient density one can now calculate the density distribution. By stacking the reconstructed planes on top of each other, one obtains a measurement volume, which contains the 3D density distribution inside the free jet.

### 4 Results

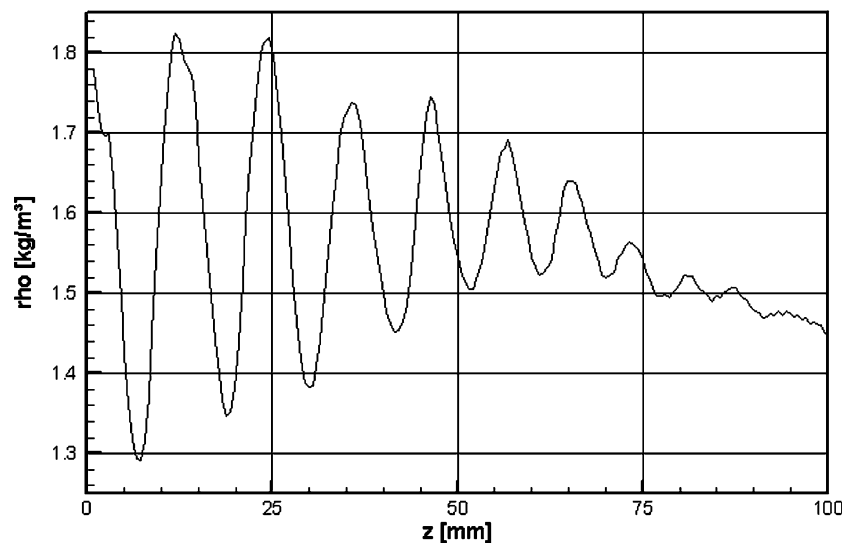
The result of the reconstruction of the double free jet is shown in Fig. 9. Figure 9a shows a slice along the jet axis at a position of  $x = 0$  mm, the Fig. 9b, c show slices at the positions  $z = 4.5$  and  $z = 11.5$  mm, respectively. The distance between data points is 0.3 mm. The jet is under-expanded and shows the density fluctuation which is typical for this type of flow.

Figure 10 shows the density distribution in the core of the bigger jet along the  $z$ -coordinate at  $x = 0$  mm and  $y = 4.5$  mm. Assuming isentropic conditions, it is possible to calculate the density at the nozzle exit to be  $1.90 \text{ kg/m}^3$ . In Fig. 9 the measured density at the Nozzle exit amounts



**Fig. 9** a Density distribution in the center slice at  $x = 0$  mm. b Density in a slice at  $z = 4.5$  mm. c Density in a slice at  $z = 11.5$  mm

**Fig. 10** Density at  $x = 0$  mm,  $y = 4.5$  mm,  $z$





to a maximum of  $1.85 \text{ kg/m}^3$  which is 2.6% lower than from the isentropic calculation expected. However it should be pointed out, that the values directly adjacent to the nozzle exit are disturbed by the shadow which the nozzle casts on the images. This disturbance can be seen in Fig. 9a and Fig. 10.

## 5 Conclusion

The background oriented schlieren method has successfully been used together with a tomographic reconstruction algorithm to determine the density distribution in a under-expanded free jet of air out of a double hole orifice. The projections of the density field in 36 directions are taken with one camera. The reconstruction is done using filtered back projection and the mean values of the integrated refractive index gradients in each projection direction. The reconstructed 3D density field shows the typical diamond structure of the density distribution in under-expanded free jets with good resolution. In contrast to the work of Venkatakrishnan (2004) here the Density gradients were used directly for the tomographic reconstruction. In advance to the experiments the properties of the background oriented schlieren method (BOS) regarding sensitivity, accuracy and resolution have been investigated. The sensitivity depends mainly on the geometry of the set-up, the camera resolution and the evaluation algorithm. It rises with larger focal length of the camera, a position of the density field near to the camera and a camera with higher resolution as well as with smaller detectable pixel shifts. In contrast the overall length of the set-up plays a minor role. For the assessment of the accuracy of the BOS method, the density field of thermally stable stratified air has been investigated. The measurements carried out with the BOS method show good agreement with the measurements using temperature sensors. The comparison also shows that the accuracy of the BOS measurement is within the error margin of the temperature sensors, even for very low values of the density gradient. The resolution of the BOS method is described by its transfer function. The transfer function is determined assuming that the apparent pixel shift is averaged over the interrogation window size. Analysis shows that only the mean value of the shift in a projection is measured correctly.

The present work quantifies accuracy, resolution, and sensitivity of the BOS method and shows its applicability to a complex 3D flow. For unsteady flows, however, the next step must be simultaneous measurements by several cameras.

**Acknowledgments** Funding from Deutsche Forschungsgemeinschaft under grant Se 1023/3-2 and Ko 1718/6-2 is gratefully acknowledged. The authors gratefully acknowledge one anonymous reviewer's advice for the simplification of Eq. 8.

## References

- Augenstein E, Leopold F, Richard H, Raffel M (2001) Schlieren techniques in comparison: the background oriented schlieren method versus visualization with holographic filters, 4th international symposium on particle image velocimetry, Göttingen, Germany
- Kak AC, Slaney M (1988) Principles of computerized tomographic imaging. IEEE Press, New York (1989)
- Blinkov GN, Fomin NA, Soloukhin MN, Vitkin DE, Yadrevskaya NL (1989) Speckle tomography of a gas flame. *Exp Fluids* 8:72
- Dalziel B, Hughes GO, Sutherland BR (2000) Whole-field density measurements by 'synthetic schlieren'. *Exp Fluids* 28(4):322–335
- Elsinga E, Oudheusden BW, Scarano F, Watt DW (2004) Assessment and application of quantitative schlieren methods: calibrated color schlieren and background oriented schlieren. *Exp Fluids* 36(2):309–325
- Faris G, Byer R (1988) Three-dimensional beam-deflection optical tomography of a supersonic jet. *Appl Optics* 27(24):5202–5212
- Formin NA (1997) Speckle photography for fluid mechanics. Springer, Germany pp 195–197
- Klinge F, Kirmse T, Kompenhans J (2003) Application of quantitative background oriented schlieren (BOS): investigation of a wing tip vortex in a transonic windtunnel. *Proceedings of PSFVIP-4*, F4097. Charmonix, France
- Meier G E A (1999) Hintergrundschlierenverfahren, Deutsche Patentanmeldung, DE19942856A1
- Raffel M, Willert C E, Kompenhans J (1998) Particle image velocimetry: a practical guide. Springer, Germany
- Meinhart CD, Wereley ST, Santiago JG (2000) A PIV algorithm for estimating time-averaged velocity fields. *ASME J Fluids Eng* 122(2):285–289
- Natterer F (1986) The mathematics of computerized tomography. Wiley, USA
- Richard H, Raffel M, Rein M, Kompenhans J, Meier GEA (2000) Demonstration of the applicability of a background oriented schlieren (BOS) method. *Proceedings 9th international symposium on applied laser techniques to Fluid Mechanics*, Lisbon, Portugal
- Rotteveel St R (1992) Optische Tomographie zur Untersuchung von Zylinderinnenströmungen. *VDI Reihe 6 Nr. 278*. VDI Verlag, Düsseldorf pp 50
- Venkatakrishnan L (2004) Density measurements in an axis symmetric underexpanded jet using background oriented schlieren technique, 24 AIAA aerodynamic measurement technology and ground testing conference, paper AIAA 2004–2603, Portland, Oregon
- Venkatakrishnan L, Meier GEA (2004) Density measurements using background oriented schlieren technique. *Exp Fluids* 37:237–247, DOI:10.1007/s00348-004-0807-1
- Nogueira J, Lecuona A, Rodriguez PA (2005) Limits on the resolution of correlation PIV iterative methods. *Fundamentals Exp In Fluids* 39:305–313, DOI 10.1007/s00348-005-1016-2